



HAL
open science

Discrete and Continuum analysis of localised deformation in sand using X-ray CT and Volumetric Digital Image Correlation

S.A. Hall, Michel Bornert, Jacques Desrues, Yannick Pannier, Nicolas Lenoir, Gioacchino Cinno Viggiani, Pierre Bésuelle

► **To cite this version:**

S.A. Hall, Michel Bornert, Jacques Desrues, Yannick Pannier, Nicolas Lenoir, et al.. Discrete and Continuum analysis of localised deformation in sand using X-ray CT and Volumetric Digital Image Correlation. *Geotechnique*, 2010, 60 (5), pp.315-322. 10.1680/geot.2010.60.5.315 . hal-00541535

HAL Id: hal-00541535

<https://hal.science/hal-00541535v1>

Submitted on 10 May 2022

HAL is a multi-disciplinary open access archive for the deposit and dissemination of scientific research documents, whether they are published or not. The documents may come from teaching and research institutions in France or abroad, or from public or private research centers.

L'archive ouverte pluridisciplinaire **HAL**, est destinée au dépôt et à la diffusion de documents scientifiques de niveau recherche, publiés ou non, émanant des établissements d'enseignement et de recherche français ou étrangers, des laboratoires publics ou privés.



Distributed under a Creative Commons Attribution - NonCommercial 4.0 International License

Discrete and continuum analysis of localised deformation in sand using X-ray μ CT and volumetric digital image correlation

S. A. HALL*, M. BORNERT†‡, J. DESRUES*, Y. PANNIER†, N. LENOIR*, G. VIGGIANI*
and P. BÉSUELLE*

The objective of this work was to observe and quantify the onset and evolution of localised deformation processes in sand with grain-scale resolution. The key element of the proposed approach is combining state-of-the-art X-ray micro tomography imaging with three-dimensional volumetric digital image correlation techniques. This allows not only the grain-scale details of a deforming sand specimen to be viewed, but also, and more importantly, the evolving three-dimensional displacement and strain fields throughout loading to be assessed. X-ray imaging and digital image correlation have been in the past applied individually to study sand deformation, but the combination of these two methods to study the kinematics of shear band formation at the grain scale is the first novel aspect of this work. Moreover, the authors have developed a completely original grain-scale volumetric digital image correlation method that permits the characterisation of the full kinematics (i.e. three-dimensional displacements and rotations) of all the individual sand grains in a specimen. The results obtained using the discrete volumetric digital image correlation confirm the importance of grain rotations associated with strain localisation.

KEYWORDS: deformation; fabric/structure of soils; failure; laboratory tests; sands

INTRODUCTION

The importance of strain localisation in soil behaviour has been known for a long time, and it has been thoroughly investigated in the laboratory. However, it should be kept in mind that in the presence of localised deformations, the meaning of stress and strain variables derived from boundary measurements of loads and displacements is only nominal, or conventional. Therefore, the most valuable experimental contributions to the understanding of localised deformation are those measuring, in one way or another, the full field of deformation in the specimen, which is the only means by which test results can be appropriately interpreted (Viggiani & Hall, 2008). Full-field analysis of strain localisation in sand started with work in the late 1960s in Cambridge (e.g. Roscoe *et al.*, 1963; Roscoe, 1970) and has been continued over the last decades in the work of a number of groups (see a review by Desrues & Viggiani (2004)). Most of these works were conducted using specifically designed plane strain devices, and used a range of full-field methods, the more advanced of which allowed observation of the

L'objectif du travail présenté était d'observer et de quantifier le processus de localisation de la déformation dans un sable, à l'échelle des grains. La clé de l'approche proposée est la combinaison de la tomographie à rayons X de dernière génération, avec la généralisation des techniques de corrélation d'images numériques aux images volumiques 3D (V-DIC). Cette approche permet non seulement d'observer les détails à l'échelle des grains pour l'ensemble d'un échantillon soumis à un processus de déformation, mais aussi et surtout de mesurer les champs de déplacement et de déformation associés, tout au long du chargement. Bien que l'imagerie X et la corrélation d'images numériques aient déjà été appliquées séparément pour l'étude de la déformation du sable, la combinaison de ces deux méthodes pour l'étude de la cinématique de formation de bande de cisaillement dans le sable observé comme milieu granulaire est inédite, et c'est le premier aspect novateur des travaux présentés ici. De plus, nous avons développé une méthode de V-DIC discrète entièrement originale, permettant de caractériser la cinématique individuelle complète (à savoir déplacements et rotations tridimensionnels) de tous les grains de sable dans l'échantillon. Les résultats obtenus en utilisant la V-DIC discrète confirment l'importance de la rotation individuelle des grains, associée à la localisation de la déformation.

specimen throughout loading by optical methods, thereby permitting measurement of the evolving strain field. In the 1960s, X-ray radiography was first used to measure two-dimensional (2D) strain fields in sand (e.g. Roscoe, 1970). From the early 1980s, X-ray tomography was used by Desrues and coworkers (Desrues, 1984; Colliat-Dangus *et al.*, 1988; Desrues *et al.*, 1996) and later by Alshibli *et al.* (2000); see Desrues (2004) for a review. These studies provided valuable three-dimensional (3D) information on localisation patterning in sand, and demonstrated the potential of X-ray tomography as a quantitative tool, for example for measuring the evolution of void ratio inside a shear band and its relation to critical state (Desrues *et al.*, 1996).

The recent advent of X-ray micro tomography, originally with synchrotron sources and now with laboratory scanners, has provided much finer spatial resolution, which opens up new possibilities for understanding the mechanics of granular media (in three dimensions) at the scale of the grain. Oda *et al.* (2004) presented micro tomography images of sand grains inside a shear band, showing organised structures that would not have been seen in standard X-ray tomography images (because of insufficient resolution) and that had only previously been observed in 2D thin sections (Oda & Kazama, 1998).

It should be noted that the images by Oda *et al.* (2004) were obtained post-mortem, that is after testing. However, a full understanding of the mechanisms of deformation, in particular localisation, can only be achieved if the entire deformation process is followed throughout a test while the

* Laboratoire 3S-R, CNRS, Université Joseph Fourier, Grenoble, France.

† LMS, CNRS, École Polytechnique, Palaiseau, France.

‡ UR Navier, École des Ponts ParisTech, Marne-la-Vallée, France.

specimen deforms. This is possible by using in-situ X-ray tomography (in situ meaning X-ray scanning at the same time as loading). A number of such in-situ studies for triaxial tests on sand have been performed using medical or industrial tomography systems (e.g. Desrues *et al.*, 1996; Alshibli *et al.*, 2000; Otani *et al.*, 2002). More recently, Matsushima *et al.* (2006, 2007) have used synchrotron X-ray in-situ micro tomography, which allowed them to identify individual sand grains and track their displacements throughout a triaxial test – note that this tracking was carried out only in two dimensions for a section through the specimen.

In the present authors' previous work 3D volumetric digital image correlation (V-DIC) has been applied to a sequence of X-ray tomography images taken during a triaxial test on a clay–rock specimen (Lenoir *et al.*, 2007). In the present paper, results are shown of a similar DIC-based analysis of deformation for a sand specimen under triaxial compression. In addition a new grain-scale V-DIC method is developed that permits the characterisation of the full kinematics (i.e. 3D displacements and rotations) of all the individual sand grains in a specimen.

The structure of the paper is as follows. First, the experimental set-up for triaxial testing with concurrent X-ray micro tomography is described. The main features of the DIC methodologies (continuum and discrete) used in this study and present results from one triaxial compression test on Hostun sand are then described. Complete 3D images of the specimen were recorded at several stages throughout the test, which were subsequently analysed using the two different V-DIC approaches. The evolution of full-field incremental kinematics (at both the continuum level and the grain scale) is presented, with special emphasis on strain localisation. Different features of localised deformation are identified at different scales and their spatial and temporal development is characterised.

EXPERIMENTAL SET-UP AND MATERIAL TESTED

The experimental results presented in this work come from a testing programme carried out at the European Synchrotron Radiation Facility (ESRF) in Grenoble on

beamline ID15A. X-ray micro tomography allows high spatial resolution (in the order of a few microns), which is crucial for understanding mechanics down to the grain scale. Using a synchrotron source also provides, thanks to the high photon flux, very fast scanning (minutes, as opposed to hours for laboratory X-ray scanners). In these experiments, acquisition times were 12 min for a scan of the entire sample.

The tests were conducted using a specifically built in-situ set-up that could be placed in the X-ray beam allowing the specimens to be scanned under load, see Fig. 1. The triaxial apparatus, made from poly(methyl methacrylate) (PMMA) (very transparent to X-rays), is practically the same as a conventional system, except the much smaller size and the shape of the confining cell. Note that the tensile reaction force is carried by the cell walls and not by tie bars (which avoids having any obstacles to the X-ray beam). The axial load and hence the deviatoric stress are applied using a motor-driven screw actuator, which also does not interfere with the tomographic X-ray scans. See Lenoir (2006) and Viggiani *et al.* (2004) for full details.

The triaxial compression test discussed herein was performed on a dry specimen of Hostun sand under a confining pressure of 100 kPa. Deviatoric loading was strain controlled, with a screw-driven piston descending at 60 $\mu\text{m}/\text{min}$, which corresponds to quite a low strain rate (0.05%/min for a 11 mm high specimen). Hostun sand is a fine-grained, angular siliceous sand with a mean grain size (D_{50}) of about 300 μm . The specimen was 11 mm in diameter, 22 mm high and had an initially dense packing. It should be noted that despite the small sample size (in comparison to standard triaxial tests on sands), the specimen can be considered large enough to be mechanically pertinent (i.e. its response can be considered representative of that of a larger mass of the material); in fact the sample comprises roughly 50 000 grains. These reduced dimensions were imposed by the X-ray imager width, which was just 14 mm (the sample needed to be smaller than this in order not to risk passing out of the field of view, although this does occur by the end of the test; see later). The spatial resolution (i.e. the voxel size) was set to $14 \times 14 \times 14 \mu\text{m}^3$, which was enough to

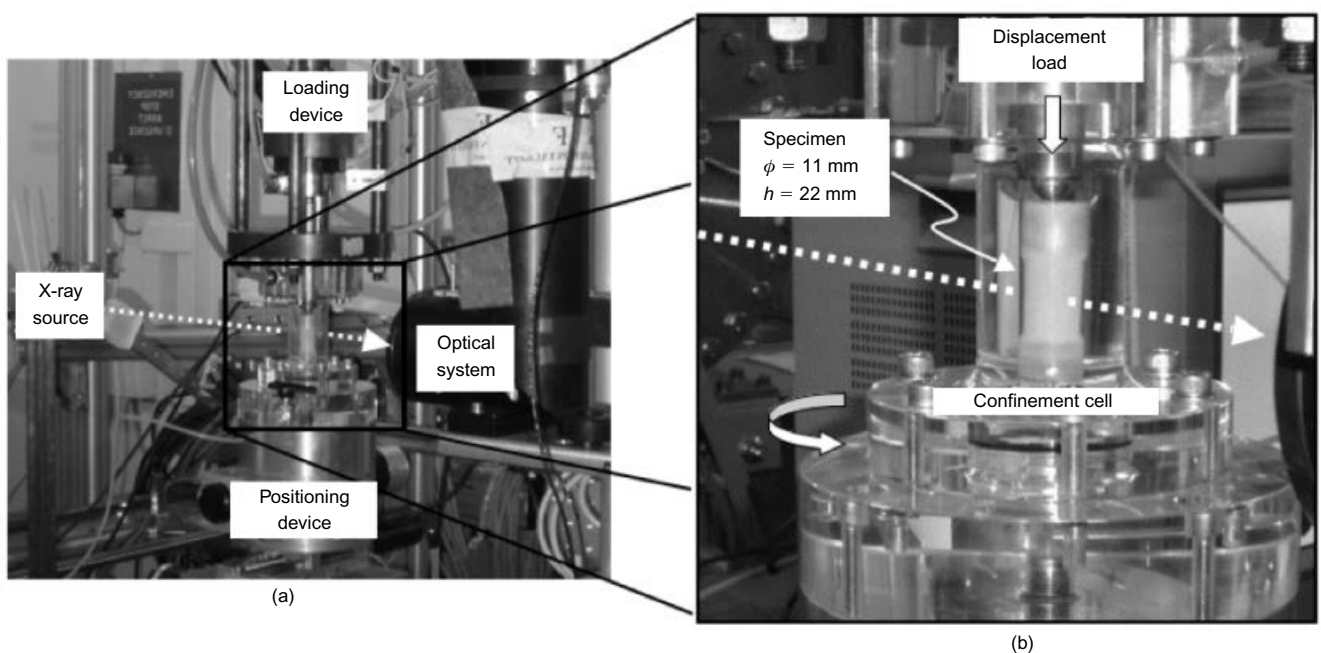


Fig. 1. Tomography set-up for triaxial testing at the beam-line ID15A at ESRF. (a) Complete set-up on the beam-line and (b) zoom on the specimen inside the triaxial cell

identify clearly the individual grains (recall that the mean grain size is around 300 μm or 21 voxels; each grain contained about 5500 voxels in the tomography images).

CONTINUUM AND DISCRETE VOLUMETRIC DIGITAL IMAGE CORRELATION

Surface full-field strain measurement by digital image correlation (DIC) techniques was pioneered in the 1980s (e.g. Sutton *et al.*, 1983; Chu *et al.*, 1985). The availability of increasingly efficient optical sensors and the increase of computer power (at a much lower cost) have made DIC techniques almost standard in experimental mechanics. Numerous applications have been reported for a wide range of materials and structures, loading conditions, scales and imaging techniques, see for example the recent review by Withers (2008). DIC can be used to determine surface displacements and strains in two dimensions using a single camera, or in three dimensions using two cameras (stereo-vision and stereo-correlation, where out-of-plane surface displacements can be measured, see Orteu (2009)). The extension of DIC to measure displacement and strain fields within solid objects, for example using 3D images acquired by X-ray tomography, is more recent (e.g. Bay *et al.*, 1999; Bornert *et al.*, 2004; Verhulst *et al.*, 2004; Lenoir *et al.*, 2007; also see Bay (2008) for a review).

The theoretical formulation of *volume* DIC is a straightforward extension of *surface* DIC. Whatever dimension (2D or 3D), DIC is a mathematical tool to define the best mapping of an image into another. More precisely, the aim is to determine the transformation Φ that relates reference and deformed configurations of an evolving system. The method is based on the fundamental assumption that at any point x the grey levels in the first image, $f(x)$, are convected into the grey levels of the second image, $g(x)$, by the transformation Φ , that is, $g(\Phi(x)) = f(x)$. In practice this relation is never fully satisfied, because of systematic and random noise. For the case of images acquired by X-ray micro tomography, random noise can be high and systematic reconstruction artefacts are often present.

Implementations of DIC usually involve local evaluations of the transformation Φ over cubic (for the volume case) subsets that are regularly distributed over the reference image. The evaluation requires solving an optimisation problem for each subset, in which essentially some measure of the similarity of $f(x)$ and $g(\Phi(x))$ in the considered subset is maximised over a parametric set of transformations. As a digital image is a discrete representation of grey levels, any integral over subsets is in fact discretised into a sum over *voxels* (the 3D version of pixels). Some interpolation is therefore necessary to evaluate the transformation with sub-voxel accuracy.

It should be noted that standard implementations of the approach described above assume a continuous displacement field, at least within each subset. Locally, the transformation is assumed to be a rigid translation, or a low-order (usually linear or quadratic) polynomial expansion of the actual transformation. When deriving strain from the displacements of separate subsets, continuity between subsets is assumed. For this reason, this DIC analysis is referred to as ‘continuum DIC’. Such a procedure can be applied to study the deformation of a granular material such as sand as long as the spatial scale of the investigation remains large with respect to the grain size. It may also be used at somewhat smaller scales (a few grains within the correlation subsets) under the condition that only small deformation increments are considered. However, a different DIC approach is possible, which recognises the granular character both of the images and the mechanical response, and has therefore the

specific objective of investigating the kinematics of *individual* sand grains. In this work, a ‘discrete DIC’ procedure has been developed with the specific aspect that the regularly shaped and spaced subsets are replaced by subsets centred on each individual grain, with a shape following the actual shape of the grain. In practice, the subsets include a grain plus a small surrounding layer a few voxels thick (the reason for this layer is that, possibly because of the relatively high noise level in the X-ray images and an almost uniform X-ray absorption of the sand grains, the grey level variation within a grain was not enough for DIC; adding a layer provided the extra information of grain shape, which is characteristic of each individual grain). If the grains are assumed to be rigid, then the transformation of each subset is a rigid motion, that is it involves a three-component translation vector plus a rotation. The latter is represented by a rotation axis and a positive angle of rotation about this axis (the axis is parameterised by two polar angles, a longitude with respect to the specimen axis, and a latitude in the cross-sectional plane).

The practical implementation of this discrete DIC comprises the following four consecutive steps.

- (a) The image of the undeformed specimen is segmented in order to identify and label individual grains. This is performed using a watershed algorithm in the image-processing package *visilog* (copyright Noesis, see <http://www.noesisvision.com/>).
- (b) A mask is defined for each grain, covering the grain plus a three-voxel wide layer around the grain. This was implemented within the code *CMV-3D* (Bornert *et al.*, 2004) using the *ITK* image-processing library (see <http://www.itk.org/>).
- (c) Standard DIC procedures of *CMV-3D* are applied to determine a first evaluation of the translation of each grain, making use of sufficiently large cubic subsets centred on the grains.
- (d) Starting from these initial estimates, the translation and rotation of each grain are determined using the discrete DIC algorithm, that is by applying optimisation to the subsets defined in step (b). Also this step has been integrated into the *CMV-3D* software, using the generic registration algorithms in *ITK*.

The final output of the discrete DIC procedure is a set of six transformation parameters for each grain. As an indication of the computational cost of this procedure: step (a) took about 7 h to extract about 50 000 grains from an 8 bit $900 \times 900 \times 1542$ image; step (b) took about 45 min, while steps (c) and (d) took slightly less than 1 s per grain, on a Linux-based workstation with a 2.3 GHz Xeon processor. Memory-wise, step (c) required about 3 Gb internal memory, whereas more than 8 Gb were needed for step (d). Note that several deformation steps can be run concurrently, therefore in principle the entire test could be processed in about 24 h on a dual-quadricore computer with enough memory (64 Gb).

In the following, the results obtained using both continuum and discrete V-DIC are presented. The former uses the code *TomoWarp*, which is based on the work of Hall (2006) (see Hall *et al.* (2010) for a 2D application to a granular material). Discrete V-DIC has been integrated into *CMV-3D*, a code developed by Bornert *et al.* (2004) (see also Lenoir *et al.* (2007) for further details and an application to geomechanics).

SELECTED RESULTS

X-ray tomography scans were carried out at key moments throughout the test, which are marked by (small) relaxations

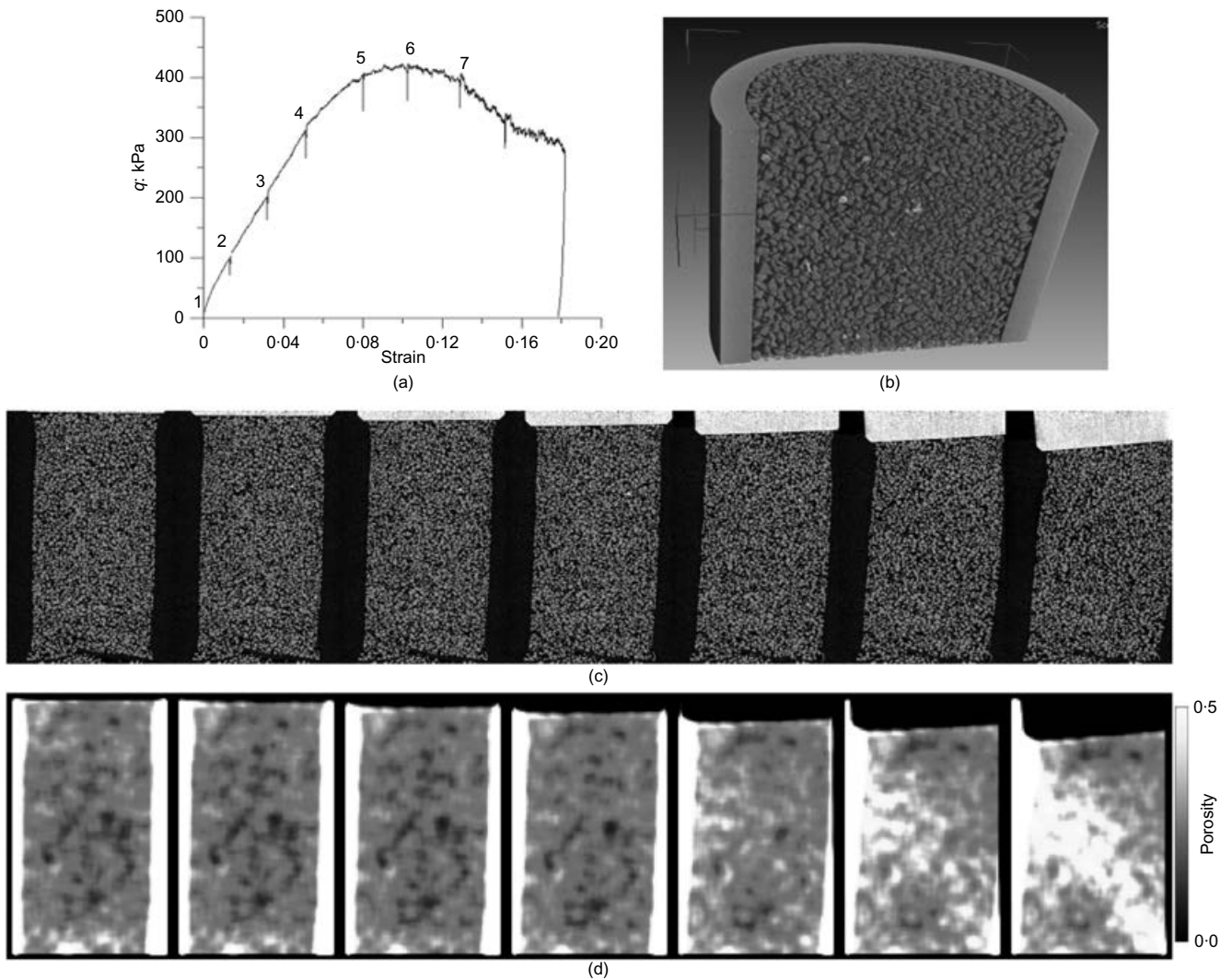


Fig. 2. (a) Deviator stress plotted against axial strain curve for the deviatoric loading part of the triaxial compression test. (b) 3D rendering of a specimen of Hostun sand showing the grain detail. (c) Vertical slices extracted from the seven 3D X-ray micro tomography images of the sand specimen acquired throughout the triaxial compression. (d) Equivalent slices through the 3D volumes of calculated porosity. For scale, note that the initial sample diameter was 11 mm

in the loading curve in Fig. 2(a). The sample stress–strain response shows a roughly linear initial trend followed by a curvature to the peak stress at around 11% nominal axial strain, after which the stress drops, to what is probably the beginning of a plateau, after which the test was stopped and the sample unloaded.

Figure 2(b) shows the grain detail which is possible to obtain for Hostun sand through X-ray tomography. For the sake of clarity, in the following only 2D slices through this volumetric data and the subsequent V-DIC results are shown. Fig. 2(c) shows a series of vertical slices through the X-ray tomography images at different stages in the test (see Fig. 2(a)). These slices, which are roughly perpendicular to the planar band of localised strain that developed during the test, show that the specimen gradually leans to one side, with a rotation of the upper platen in the latter part of the test. However, there is no clear evidence of localised deformation in these images. Porosity maps shown in Fig. 2(d) were obtained from the grey-scale images based on overlapping cubic windows of side 61 voxels (854 μm) throughout the sample volume. From these porosity fields an evolving inclined zone of localised dilatancy can be seen.

Continuum V-DIC has been carried out on consecutive pairs of 3D images to provide the incremental displacement

and strain fields (the results are thus averages over the given time interval). The key DIC parameters are the distances between the calculation nodes (which also represent the reference length for subsequent strain calculation) and the correlation window sizes; in this analysis these were, respectively, 20 voxels (or 280 μm) and a cube with sides of 21 voxels (or 294 μm) reduced to 11 voxels (or 154 μm) for the sub-voxel derivation. Results from this analysis indicate that, despite the granular nature of the material, smooth and relatively continuous displacement fields are measured. Fig. 3 shows vertical slices through the 3D field of maximum shear strain $(\epsilon_1 - \epsilon_3)/2$ (where ϵ_1 and ϵ_3 are the major and minor principal strains) for increments 3–4, 4–5, 5–6 and 6–7. These strain images clearly show the evolution of a localised band that traverses the sample diagonally from left to right. It is worth noting that this is an incremental analysis, indicating that the deformation is active in each strain increment. This is different from what can be seen with accumulated porosity changes shown in Fig. 2(d). As such it is seen from these incremental maps that the localisation possibly initiated in increment 4–5, and was clearly developed in 5–6, that is before the peak load. Note that localisation is visible in these maps before it becomes clear in the porosity images (Fig. 2(d)). The general picture is of a localisation of shear strain and dilatancy which starts as a broad zone and

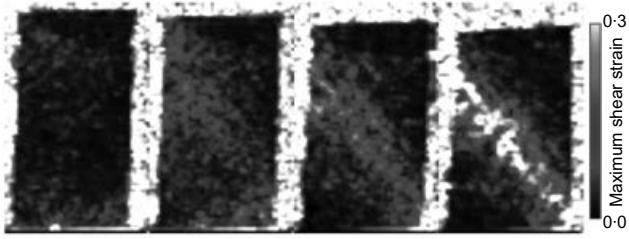


Fig 3. Continuum V-DIC derived incremental maximum shear strains (as defined in text) for increments 3–4, 4–5, 5–6 and 6–7 (previous increments showed much the same picture as 3–4). The images show vertical slices through the shear strain volume near the middle of the specimen at an equivalent position to Fig. 2

then progressively thins with loading. In increment 6–7, this zone has a width of about 5 mm (i.e. about $17 D_{50}$). It is also clear that the localised zone is not uniform, showing a degree of structure.

Discrete V-DIC has been applied to provide incremental analysis of grain kinematics. Following the procedure detailed earlier, a set of six scalar quantities (three displacements and three rotations) describing the kinematics of each sand grain are determined. From these results, displacement components at any position within a grain can be deduced. As an example, in Fig. 4 the field of incremental vertical displacements is viewed in three orthogonal slices through the volume for increment 3–4, before the onset of localisation, and increment 6–7, when a shear band is well developed in the specimen – as clearly portrayed in all three viewing planes. Despite these results having been derived from a discrete analysis, they indicate a relatively continuous field of displacements, even in the presence of strain localisation, which explains why continuum V-DIC performs well. However, locally the field can be discontinuous, as discussed later.

Figure 5(a) shows a 3D view of the rotation vectors for each grain in increments 3–4, 4–5, 5–6 and 6–7. Fig. 5(b) shows, for the same increments, the magnitude of rotation for each grain about its rotation axis (recall this is specific for a grain) in a vertical slice corresponding to the middle of the specimen, as in Fig. 3. Note that the grains in Fig. 5(b) are represented in the configuration that existed

at the beginning of the test, and not in their displaced positions. Both sets of images in Fig. 5 indicate that grain rotations become progressively more intense into a zone that roughly corresponds to where shear strain localises (see Fig. 3).

DISCUSSION AND CONCLUSIONS

The objective of this work was to observe and quantify the onset and evolution of localised deformation processes in sand with grain-scale resolution. The key element of the proposed approach is combining state-of-the-art X-ray micro tomography imaging with 3D V-DIC techniques. This makes it possible not only to view the grain-scale details of a deforming sand specimen, but also and more importantly to assess the evolving 3D displacement and strain fields throughout loading. While X-ray imaging and DIC have been in the past applied individually to study sand deformation, the combination of these two methods to study the kinematics of shear band formation at the scale of the grains is the first novel aspect of this work. Moreover, a completely original grain-scale V-DIC method has been developed that permits the characterisation of the full kinematics (i.e. 3D displacements and rotations) of all the individual sand grains in a specimen.

The application of continuum V-DIC has allowed the development of a localised shear band to be characterised throughout a test. Incremental analysis of consecutive steps reveals that strain localisation begins before the peak stress, and indicates a diffuse, wide band progressively thinning to a $17 D_{50}$ wide band after peak. It also appears that the shear band contains a narrower internal core of much higher strain, and that within the band there are aligned zones of either reduced or elevated strains at angles ‘conjugate’ to the main band direction.

The results obtained using the discrete V-DIC confirm the importance of grain rotations associated to strain localisation. A clear correspondence can be established between the zones of the specimen experiencing localisation of (continuum) shear strain and the zones where grain rotations are more intense. Fig. 6 shows the history of rotation throughout the test for a few selected grains, indicating contrasting behaviour for grains positioned inside and outside the region where shear strain localises. Grains inside the band show a rapid acceleration of rotation as the shear band initiates,

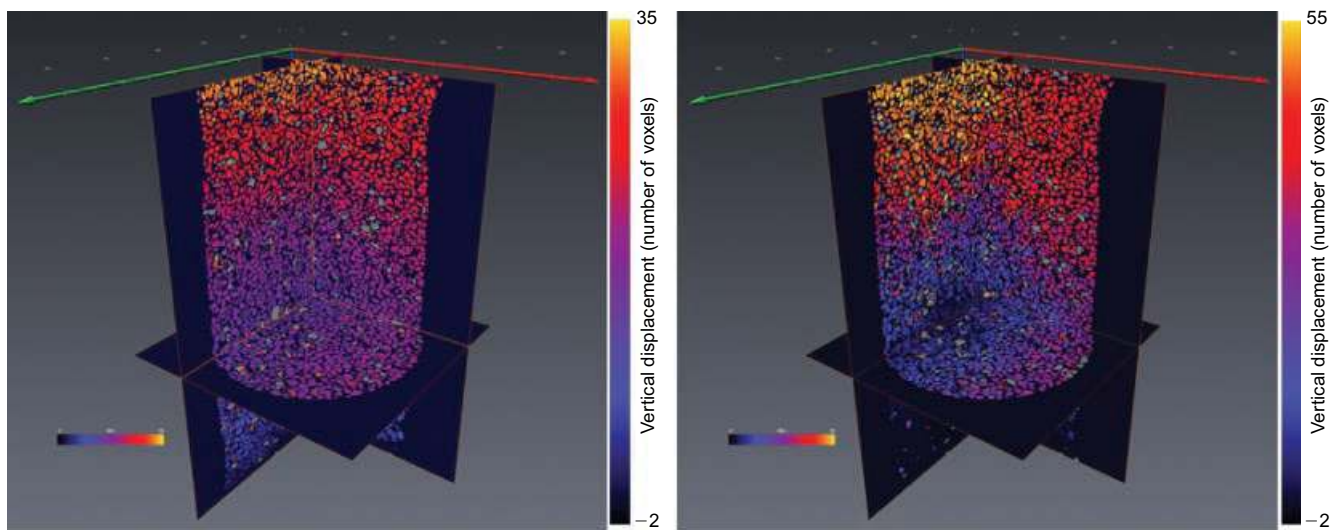


Fig 4. Discrete V-DIC derived grain displacements (vertical component) viewed in three orthogonal slices through the volume for strain increments 3–4 and 6–7 (before and after peak stress, respectively). Grains coloured grey are those for which the image correlation was not successful (about 2% and 5% of the grains for 3–4 and 6–7, respectively)

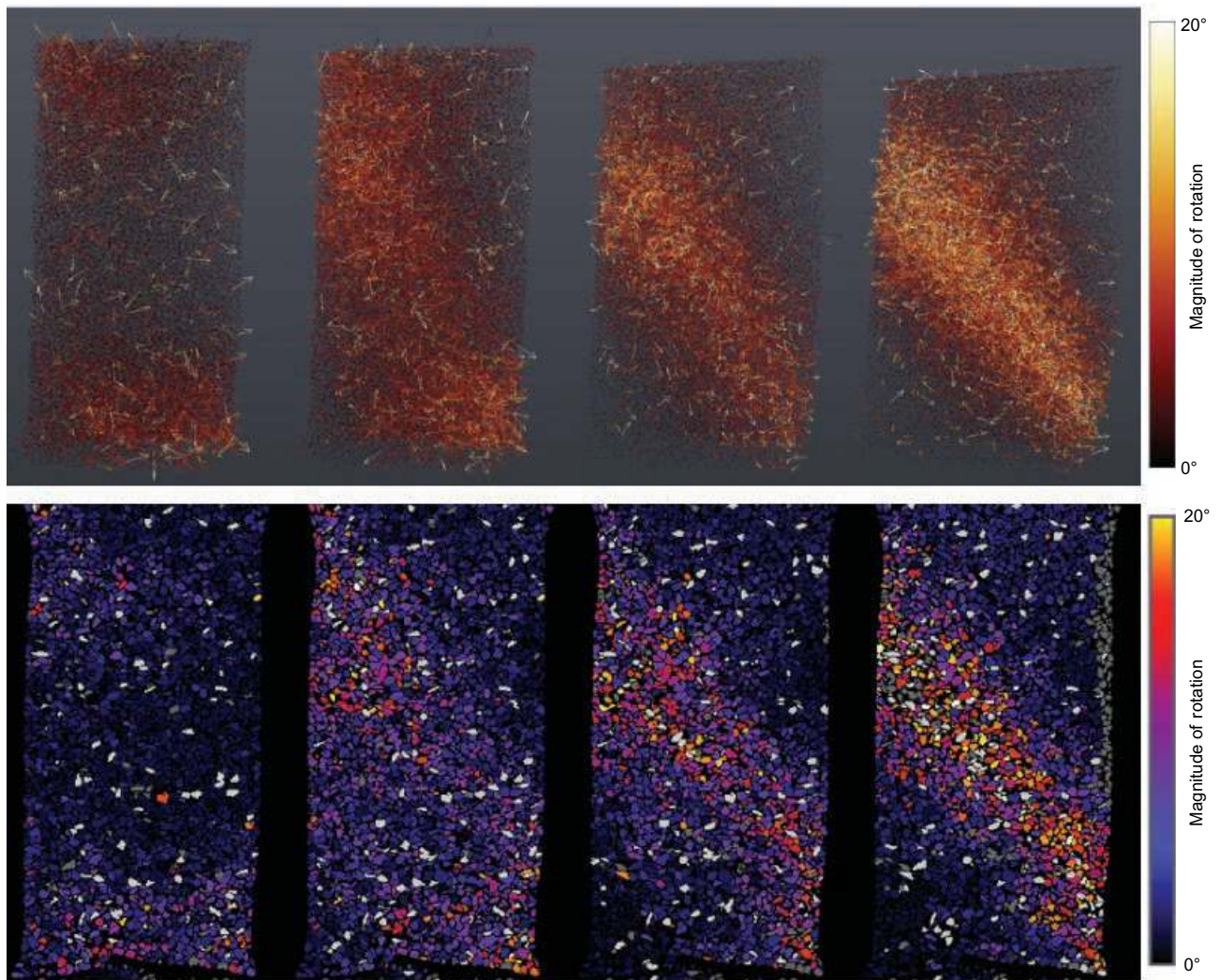


Fig 5. Discrete V-DIC derived incremental grain rotations for increments 3–4, 4–5, 5–6 and 6–7 (previous increments showed much the same picture as 3–4). Top: 3D volume view of the rotation vectors (axes of rotation for each grain are plotted with their length and colour indicating the magnitude of the rotation about these axes). Bottom: magnitude of the grain rotations plotted for vertical slices through the middle of the specimen at an equivalent position to Figs 2 and 3; note that the grains are plotted in the configuration at the start of the test for all increments. Grains coloured grey are those for which the image correlation was not successful and those coloured white are those with a rotation above a threshold value of 20° (corresponding also to the long white vectors in the upper images)

whereas grains elsewhere show relatively constant increase of rotation as the test progresses.

Figure 7 shows the discrete V-DIC vertical component of total displacement from start to image 7 (note that these displacements include the contribution due to the grain rotations). The overall impression from the left image in the figure is that discrete V-DIC yields a relatively continuous displacement field, even at this stage of the test when strain localisation has developed. However, the zoomed images reveal that local discontinuities exist at the scale of the grains. While only a few such examples of discontinuities are noted in the figure, it is clear that a deeper analysis of continuities/discontinuities at grain contacts and their evolution is now possible, and will be investigated in future work. It should also be noted that the grain images in Fig. 7 are those resulting from image segmentation, that is grains that are in contact will not appear so as they have been artificially separated. Therefore, it is not possible to differentiate from such segmented images grains that are in contact from those that are not. A more detailed study of grain contact evolution in space and time would require defining contacts based on the original, non-segmented images.

In constitutive modelling, it is necessary to understand the physics governing material behaviour – from the micro scale to the continuum scale. This is particularly true when modelling emergent fine-scale mechanisms whose characteristic length scales are only a few particles wide, for example shear bands. Since their initial development by Cundall & Strack (1979), discrete element methods have been gaining popularity as a numerical means to explore the mechanical behaviour of sand and other granular media at the scale of the grains. On the experimental side, micro mechanics studies are few in number, and most of them are restricted either to two dimensions or to artificial granular media such as glass beads. The few experimental studies exploring sand deformation at the scale of the grains have provided limited quantitative information so far. With the tools presented in this paper, the capability has now been provided to capture experimentally and at a pertinent level of resolution the details of grain-scale processes, including those that underlie the localisation phenomena of interest here. However, the potential of the approach has still to be fully exploited. Future directions of this research include more detailed analysis of: kinematics across grain contacts

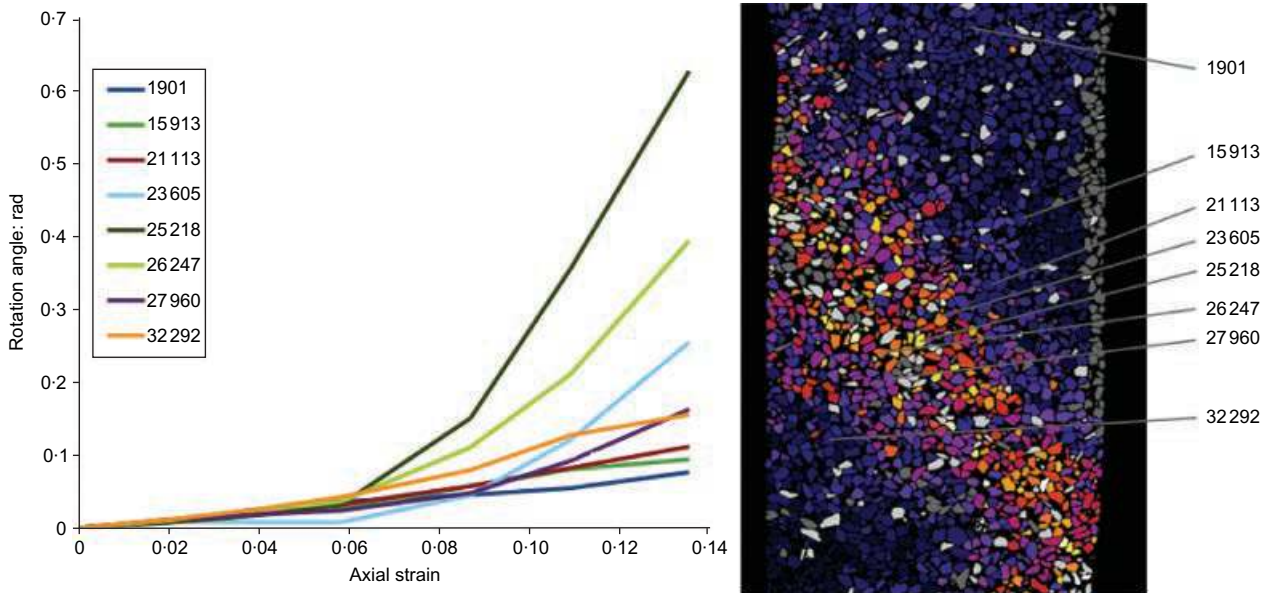


Fig 6. History of rotation for a few selected grains positioned inside and outside the localised deformation band – left: plot of total rotations for each selected grain as a function of nominal axial strain of the specimen; right: the selected grains indicated on the slice of incremental rotation for step 6–7, as in Fig. 5

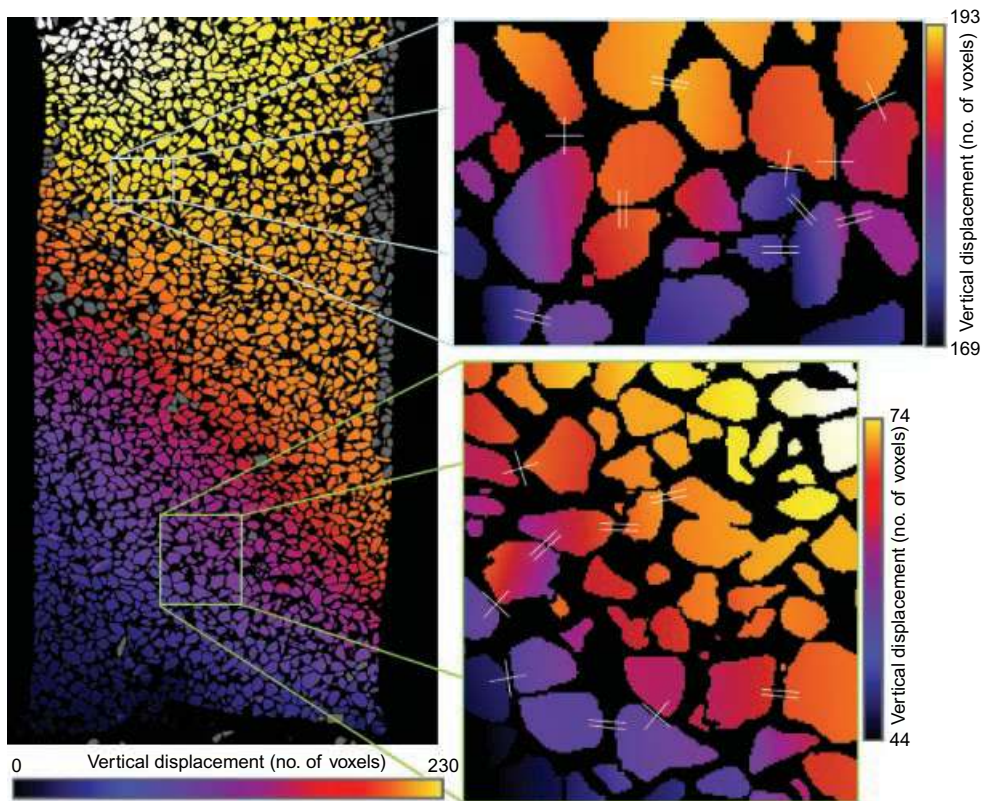


Fig 7. Vertical slice (as in previous figures) through the total z component displacement field up to image 7 from the discrete V-DIC with displacements derived at all points, within the grains, from the grain displacements and rotations. While the displacement field appears relatively continuous, the zoomed images (right) highlight that locally there exists both continuity and discontinuity of displacements between adjacent grains, as indicated by = and + respectively

and its evolution with strain localisation at the macro scale; emergence of grain-scale structures inside a shear band (e.g. the ‘columns’ of aligned grains observed by Oda *et al.* (2004) and also advocated by Rechenmacher (2006) based on continuum 2D DIC); organised kinematics, in particular grain rotation, at the onset of shear banding and through its evolution.

ACKNOWLEDGEMENTS

This work was carried out within the framework of the project MicroModEx funded by the French research agency, ANR (contract number: ANR-05-BLAN-0192). The authors acknowledge Christophe Rousseau (Laboratoire 3S-R) and Marco di Michel (ESRF), for their contributions to the experimental programme.

REFERENCES

- Alshibli, K. A., Sture, S., Costes, N. C., Franck, M. L., Lankton, M. R., Batiste, S. N. & Swanson, R. A. (2000). Assessment of localized deformation in sand using X-ray computed tomography. *Geotech. Testing J.* **23**, 274–299.
- Bay, B. K. (2008). Methods and applications of digital volume correlation. *J. Strain Anal.* **43**, 745–760.
- Bay, B. K., Smith, T. S., Fyhrie, D. P. & Saad, M. (1999). Digital volume correlation: three-dimensional strain mapping using X-ray tomography. *Expl Mech.* **39**, No. 3, 217–226.
- Bornert, M., Chaix, J. M., Doumalin, P., Dupré, J. C., Fournel, T., Jeulin, D., Maire, E., Moreaud, M. & Moulinec, H. (2004). Mesure tridimensionnelle de champs cinématiques par imagerie volumique pour l'analyse des matériaux et des structures. *Instrum Measmt Metrology* **4**, 43–88.
- Chu, T. C., Ranson, W. F., Sutton, M. A. & Peters, W. H. (1985). Applications of digital-image-correlation techniques to experimental mechanics. *Expl Mech.* **25**, No. 3, 232–244.
- Colliat-Dangus, J. L., Desrues, J. & Foray, P. (1988). Triaxial testing of granular soil under elevated cell pressure. *Proceedings of a conference on advanced triaxial testing for soil and rocks* (eds R. T. Donaghe, R. C. Chaney and M. L. Silver), STP977, pp. 290–310. Philadelphia: American Society for Testing and Materials.
- Cundall, P. A. & Strack, O. D. L. (1979). A discrete numerical model for granular assemblies. *Géotechnique* **29**, No. 1, 47–65, doi: 10.1680/geot.1979.29.1.47.
- Desrues, J. (1984). *La localisation de la déformation dans les matériaux granulaires*. PhD thesis, USMG and INPG, Grenoble, France.
- Desrues, J. (2004). Tracking strain localization in geomaterials using computerized tomography. *Proc. 1st Int. Workshop X-ray Tomography for Geomater., Kumamoto, Japan* **1**, 15–41. Lisse, The Netherlands: Balkema.
- Desrues, J., Chambon, R., Mokni, M. & Mazerolle, F. (1996). Void ratio evolution inside shear bands in triaxial sand specimens studied by computed tomography. *Géotechnique* **46**, No. 3, 529–546, doi: 10.1680/geot.1996.46.3.529.
- Desrues, J. & Viggiani, G. (2004). Strain localization in sand: an overview of the experimental results obtained in Grenoble using stereophotogrammetry. *Int. J. Numer. Analyt. Methods Geomech.* **28**, No. 4, 279–321.
- Hall, S. A. (2006). A methodology for 7D warping and deformation monitoring using time-lapse seismic data. *Geophysics* **71**, No. 4, O21–O31.
- Hall, S. A., Muir Wood, D., Ibraim, E. & Viggiani, G. (2010). Localised deformation patterning in 2D granular materials revealed by digital image correlation. *Granular Matter* **12**, No. 1, 1–14.
- Lenoir, N. (2006). *Comportement mécanique et rupture dans les roches argileuses étudiés par micro tomographie à rayons X*. PhD thesis, University of Grenoble, France (<http://tel.ccsd.cnrs.fr/tel-00011996>).
- Lenoir, N., Bornert, M., Desrues, J., Bésuelle, P. & Viggiani, G. (2007). Volumetric digital image correlation applied to X-ray micro tomography images from triaxial compression tests on argillaceous rocks. *Strain* **43**, No. 3, 193–205.
- Matsushima, T., Uesugi, K., Nakano, T. & Tsuchiyama, A. (2006). Visualization of grain motion inside a triaxial specimen by micro X-ray CT at SPring-8. In *Advances in X-ray tomography for geomaterials* (eds J. Desrues, G. Viggiani and P. Bésuelle), pp. 35–52. London: ISTE.
- Matsushima, T., Katagiri, J., Uesugi, K., Nakano, T. & Tsuchiyama, A. (2007). Micro X-ray CT at SPring-8 for granular mechanics. In *Soil stress–strain behavior: measurement, modeling and analysis* (eds H. I. Ling, L. Castillo, D. Leshchinsky and J. Koseki), pp. 225–234. The Netherlands: Springer.
- Oda, M. & Kazama, H. (1998). Microstructure of shear band and its relation to the mechanism of dilatancy and failure of granular soils. *Géotechnique* **48**, No. 4, 465–481, doi: 10.1680/geot.1998.48.4.465.
- Oda, M., Takemura, T. & Takahashi, M. (2004). Microstructure in shear band observed by microfocus X-ray computed tomography. *Géotechnique* **54**, No. 8, 539–542, doi: 10.1680/geot.2004.54.8.539.
- Orteu, J. J. (2009). 3-D computer vision in experimental mechanics. *Optics and Lasers in Engineering* **47**, No. 3–4, 282–291.
- Otani, J., Mukunoki, T. & Obara, Y. (2002). Characterization of failure in sand under triaxial compression using an industrial X-ray scanner. *Int. J. Phys. Modelling Geotech.* **2**, No. 1, 15–22.
- Rechenmacher, A. L. (2006). Grain-scale processes governing shear band initiation and evolution in sands. *J. Mech. Phys. Solids* **54**, No. 1, 22–45.
- Roscoe, K. H. (1970). The influence of strains in soil mechanics. *Géotechnique* **20**, No. 2, 129–170, doi: 10.1680/geot.1970.20.2.129.
- Roscoe, K. H., Arthur, J. R. F. & James, R. G. (1963). The determination of strains in soils by an X-ray method. *Civ. Engrg Public Works Rev.* **58**, No. 7, 873–876 and No. 8, 1009–1012.
- Sutton, M. A., Wolters, W. J., Peters, W. H., Ranson, W. F. & McNeill, S. R. (1983). Determination of displacements using an improved digital correlation method. *Image and Vision Comput.* **1**, No. 3, 133–139.
- Verhulp, E., van Rietbergen, B. & Huiskes, R. (2004). A three-dimensional digital image correlation technique for strain measurements in microstructures. *J. Biomech.* **37**, No. 9, 1313–1320.
- Viggiani, G. & Hall, S. A. (2008). Full-field measurements, a new tool for laboratory experimental geomechanics. Keynote paper. *Proc. 4th Int. Symp. Deformation Characteristics Geomater.* (eds S. E. Burns, P. W. Mayne and J. C. Santamarina) **1**, 3–26. Atlanta: IOS Press.
- Viggiani, G., Lenoir, N., Bésuelle, P., Di Michiel, M., Marelli, S., Desrues, J. & Kretschmer, M. (2004). X-ray micro tomography for studying localized deformation in fine-grained geomaterials under triaxial compression. *C. R. Mécanique* **332**, No. 10, 819–826.
- Withers, P. J. (2008). Strain measurement by digital image correlation. *Strain* **44**, No. 6, 421–422.